www.elsevier.com/locate/dsri

Biogenic silica cycling during summer phytoplankton blooms in the North Pacific subtropical gyre

Jeffrey W. Krause, Mark A. Brzezinski, Tracy A. Villareal, Cara Wilson

PII: S0967-0637(12)00184-7
DOI: http://dx.doi.org/10.1016/j.dsr.2012.09.002
Reference: DSRI2140

To appear in: *Deep-Sea Research I*

Received date: 11 May 2012
Revised date: 4 September 2012
Accepted date: 5 September 2012

Cite this article as: Jeffrey W. Krause, Mark A. Brzezinski, Tracy A. Villareal and Cara Wilson, Biogenic silica cycling during summer phytoplankton blooms in the North Pacific subtropical gyre, *Deep-Sea Research I,* http://dx.doi.org/10.1016/j.dsr.2012.09.002

Biogenic silica cycling during summer phytoplankton blooms in the North Pacific subtropical gyre

Jeffrey W. Krause [a*], Mark A. Brzezinski [a,b], Tracy A. Villareal [c], Cara Wilson [d]

[a]Marine Science Institute, University of California, Santa Barbara, California
[b]Department of Ecology Evolution and Marine Biology, University of California, Santa Barbara, California
[c]Marine Science Institute and the Department of Marine Science, The University of Texas, Austin, Port Aransas, Texas
[d]NOAA/NMFS/SWFSC Environmental Research Division, Pacific Grove, California

[*]Corresponding author: jeffrey.krause@lifesci.ucsb.edu, PHONE: (805) 893-7061, FAX: (805) 893-8062

Abstract

Biogenic silica ($bSiO_2$) cycling, diatom abundance and floristics were examined within summer-period diatom blooms in the North Pacific Subtropical Gyre (NPSG) in 2008 and 2009. *Hemiaulus hauckii* was the most abundant diatom observed in an expansive (100,000 km^2) bloom near the subtropical front in the northeastern NPSG in 2008 and the small pennate diatom *Mastogloia woodiana* dominated a smaller (30,000 km^2) bloom sampled in 2009 in the gyre interior. In both blooms, the $bSiO_2$ stock and production rates were up to an order of magnitude higher relative to non-bloom areas. Remnants of a $bSiO_2$ export event was sampled in the *H. hauckii* bloom area where the export rate at 300 m exceeded that at 150 m, and was among the highest values recorded in the NPSG. The *M. woodiana* bloom was very active with specific $bSiO_2$ production rates of 0.50-0.75 d^{-1} and net $bSiO_2$ production rates were among the highest observed in any subtropical-gyre diatom bloom to date. Net silica production rates in the euphotic zone were strongly positive within blooms and near zero outside of blooms, consistent with an important role for blooms in $bSiO_2$ export. The difference in the areal extent of the *H. hauckii* and *M. woodiana* blooms was consistent with remote-sensing observations that blooms in the northeastern portion of the NPSG, near the subtropical front, are typically more extensive than those in the gyre interior near Hawaii Ocean Time-series station ALOHA. Initial estimates suggest that blooms in the northeast region produced 3 to 25 times more $bSiO_2$ in 2008 and 2009, respectively, than did blooms in the gyre interior; and due to the large areal extent these blooms, their area-integrated production of $bSiO_2$ is similar to intense diatom blooms coastal upwelling systems (e.g. Monterey Bay, Santa Barbara Channel) despite significantly lower production rates and standing stock.

Keywords: North Pacific subtropical gyre, blooms, diatoms, silica production, net silica production, export

1. Introduction

Compared to blooms in other subtropical gyres, phytoplankton blooms in the North Pacific subtropical gyre (NPSG) are different in their timing and in the hydrographic conditions under which they occur. Winter convective mixing in the NPSG is weak and regular spring blooms do not ensue; instead, phytoplankton blooms occur during summer when the upper-water column stratification is at its annual maximum and macronutrient concentrations are at their annual minimum (Wilson, 2003; Dore *et al.*, 2008; Wilson *et al.*, 2008). This situation sharply contrasts with that in the North Atlantic Subtropical Gyre (NASG) where strong winter convection typically erodes the pycnocline and entrains nutrients into the euphotic zone, thereby stimulating a regular spring bloom after water-column restratification (Sverdrup, 1953). Summer blooms in the NPSG interior show enhanced abundance of diazotrophs (e.g. *Trichodesmium*) and diatoms (Dore *et al.*, 2008; Fong *et al.*, 2008; Villareal *et al.*, 2011; 2012); however, *Trichodesmium* is rarely observed in the northeastern NPSG near the subtropical front (Venrick, 1997; Dore *et al.*, 2008) where satellite ocean color observations reveal blooms that are generally more expansive and that longer-lived than those in the gyre interior near the Hawaii Ocean Time-series (HOT) station ALOHA (Wilson, 2003; Wilson *et al.*, 2008). At least some of the blooms occurring in the northeastern gyre are dominated by diatoms (Brzezinski *et al.*, 1998; Villareal *et al.*, 2011).

Why diatom blooms in the NPSG occur during the highly oligotrophic conditions of summer remains enigmatic. Some blooms contain diatom-diazotrophic associations (DDAs, e.g. the diatom genera *Hemiaulus* or *Rhizosolenia* and the nitrogen-fixing symbiont, *Richelia*; Villareal *et al.*, 2011), suggesting that the biological input of fixed N may play a role in bloom initiation and development. Recently, it was also suggested that summer blooms in the northeastern NPSG can occur in response to increased vertical mixing due to internal wave breakdown at the 30°N "critical latitude" (Wilson, 2011). A diatom bloom also requires adequate silicic acid; relative to the nanomolar levels of inorganic N and P in the surface waters of the NSPG, the silicic-acid requirement is easily met as surface-water concentrations are typically 0.5 – 1.5 μM. There is also evidence that the diatom taxa which dominate summer blooms have very efficient Si uptake kinetics, such that ambient silicic acid concentrations of ~1 μM would support high growth rates (Brzezinski *et al.*, 1998; Krause *et al.*, 2012).

While there currently is no consensus on the factor(s) initiating summer diatom blooms in the NPSG, there is clear evidence as to their importance in annual biogeochemical budgets. This is

somewhat counter intuitive as diatom biomass during non-bloom periods at station ALOHA, as measured by biogenic silica ($bSiO_2$) concentration, is the lowest thus far observed in the global ocean (Brzezinski *et al.*, 2011). However, at the HOT station ALOHA the contribution of diatoms to new production exceeds both their contribution to autotrophic biomass and their estimated contribution to primary production (Brzezinski *et al.*, 2011), implying a disproportionately important role for diatoms in carbon export. This is especially true for summer blooms which have been estimated to account for 18% of annual new production at station ALOHA (Dore *et al.*, 2008) and recent estimates suggest that summer blooms account for 29% of the annual production of $bSiO_2$ at ALOHA (Brzezinski *et al.*, 2011). Blooms in the northeastern gyre near the subtropical front are typically longer-lived than those at or near ALOHA (Wilson *et al.*, 2008), but their role in annual biogeochemical budgets is less clear. There is also evidence for a significant role for diatoms in the export of carbon to the ocean interior at ALOHA where observations from both shallow (150 m) and deep (≥2,800 m) sediment traps show an annual summer maximum in carbon export associated with increased diatom and $bSiO_2$ export (Scharek *et al.*, 1999a; b; Karl *et al.*, 2012). To further evaluate the contribution of summer diatom blooms to silica production and organic matter cycling in the NPSG, we examined rates of gross and net silica production, diatom abundance and taxonomic composition within summer phytoplankton blooms in the NPSG.

2. Methods

2.1 Study area and sampling

The Pacific Open-Ocean Bloom (PB) cruises were conducted aboard the R/V *Kilo Moana* from 4 –19 July 2008 (PB08) and from 29 July – 12 August 2009 (PB09). Using daily-composite images from the Moderate Resolution Imaging Spectroradiometer (MODIS, http://modis.gsfc.nasa.gov), bloom regions were identified as areas with chlorophyll a (Chl *a*) concentrations ≥ 0.12 μg L^{-1}. As the feature sampled in 2008 was relatively weak, visualizing the full extent of the bloom area required the [Chl *a*] threshold value to be slightly lower than the 0.15 μg L^{-1} value used previously (Wilson *et al.*, 2008); for consistency we use the same [Chl *a*] threshold for both PB cruises. Three regions with bloom-level [Chl *a*] were sampled, one in 2008 and two in 2009. Within each bloom region, stations were classified as representing a diatom bloom condition by meeting two criteria: 1) the >10 μm size-fraction [Chl *a*] was >30%

of the total [Chl *a*] collected on a >0.4 μm filter. This threshold value represents a three-fold increase in >10 μm [Chl *a*] fraction over that present under non-bloom conditions in the gyre during summer (Villareal *et al.*, 2011), and 2) diatom numerical abundance exceeded 1,000 cells L^{-1}, consistent with threshold bloom abundances previously applied in this region (e.g., Brzezinski *et al.*, 1998; Villareal *et al.*, 2011).

During PB08 a single bloom feature was sampled near the subtropical front northeast of Hawaii (Fig. 1). The bloom was intensifying as the ship left port in Hawaii and satellite chlorophyll levels were above the 0.12 μg L^{-1} bloom threshold when the ship arrived at the bloom, but while the area was being sampled the satellite-observed chlorophyll levels fell below the bloom threshold. As a result of the declining biomass, only one of the 18 stations sampled in the area met the diatom-bloom criteria (Fig. 1). Two bloom features were sampled in 2009. In mid-June of 2009 a high chlorophyll feature developed east of Hawaii at ~26°N, 146°W (Fig. 1), but remotely-sensed chlorophyll concentrations had dropped significantly by the time of sampling in mid-July (Fig. 1). However, satellite images revealed another bloom feature developing to the north of Hawaii at ~25°N, 155°W (Fig. 1). Two stations were sampled within this feature while it was still active (or developing), and both met the bloom-station criteria. This bloom will be referred to as the active bloom from PB09 to distinguish it from observations taken in the faded bloom further to the east.

Sampling consisted of CTD casts throughout the day. Pre-dawn casts (04:00-06:00 h, local time) were done to obtain samples for nutrient concentration, Chl *a* concentration, $bSiO_2$ concentrations and $bSiO_2$ production rates. Samples for diatom abundance and composition were taken on the rate casts or on the cast immediately before/after. On additional casts during the day, all samples were collected except those for rate measurements. Due to time constraints for sampling the second bloom region examined in 2009, rate profiles at PB09 stations 22 and 23 were conducted after 6:00 h local time, but all incubations ran 24 hours to integrate through a complete photoperiod (see below). For rate measurements water samples were taken at nine depths within the euphotic zone where the percent of irradiance was determined to be 100, 59, 31, 19, 10, 6, 3.4, 0.6 and 0.1% of that just below the surface ($\%I_0$). At non-rate stations fixed sampling depths (surface: i.e. 3 – 5 m, 10, 20, 40, 60, 80, 100, 125, 140, 160 m) were used. Seawater was collected using 12 L PVC sampling bottles on a rosette equipped with a Seabird CTD and a photosynthetically active radiation sensor to determine light attenuation. Mixed layer

depths were calculated using 1-m binned CTD data based on a 0.125 kg m^{-3} change in potential density from the 0-1 m bin.

2.2. Nutrient, taxonomy, and biogenic particulate analysis

Dissolved nutrients were collected and analyzed using standard methods. Unfiltered seawater samples for [$Si(OH)_4$] determination were refrigerated at 4°C until analysis at sea using a sensitive manual colorimetric method (Brzezinski and Nelson, 1995). Nitrate (<10 nM) and soluble reactive phosphorus (<35 nM) were also taken from sampling bottles and analyzed using both high-sensitivity methods (e.g. Church *et al.*, 2009) and standard colorimetric methods (e.g. Villareal *et al.*, 2012). The nutrient data are discussed in detail elsewhere (Duhamel *et al.*, 2010; 2011; Villareal *et al.*, 2012).

Samples for biomass and diatom-assemblage measurements were analyzed by methods used previously in subtropical-gyre regions. Seawater for biogenic ($bSiO_2$) and lithogenic silica analysis was collected in 2.8 L polycarbonate bottles, filtered through 0.6 μm polycarbonate filters, and analyzed using the sequential NaOH – HF digestion procedure (Brzezinski and Nelson, 1995) with reactions carried out in Teflon® tubes which provide low and stable blanks (Krause *et al.*, 2009). Lithogenic silica concentrations were very low (e.g. 3 – 8 nmol Si L^{-1}) and are not discussed in detail. [Chl *a*] was determined for two size fractions: >0.4 μm (e.g., total phytoplankton community) and >10 μm (e.g., diatoms, dinoflagellates) by filtering 250 mL and 500 mL, respectively, through polycarbonate membrane filters, extracting in methanol, and quantifying fluorometrically without acidification (Welschmeyer, 1994). Samples for diatom abundance and taxonomy were preserved with formalin and enumerated using inverted microscopy (Villareal *et al.*, 2012).

2.3. Measurement of biogenic silica production and export rates

Measurements of gross $bSiO_2$ production rates (ρ_P) from each sampling depth were conducted in polycarbonate bottles (300 mL) using the radioisotope ^{32}Si. Each sample received 360 Bq of high specific activity $^{32}Si(OH)_4$ (>40 kBq μmol Si^{-1}) which had been cleaned of trace metals by passage through Chelex resin (BioRad). Samples were incubated on the ship deck for 24 hours in acrylic incubators, screened to the relative light level corresponding to each sample collection depth, and continuously cooled by flowing surface seawater. After incubation, all

165 silica production rate samples were processed as described in Krause et al. (2012) and ^{32}Si
166 activity was quantified using gas-flow proportional counting at secular equilibrium of ^{32}Si and its
167 daughter isotope ^{32}P (Krause *et al.*, 2011). Specific rates of silica production (V_b) were
168 calculated by normalizing ρ_P to [$bSiO_2$] as in Brzezinski and Phillips (1997). The average V_b for
169 the upper water column was calculated by vertically integrating V_b to a specific depth (e.g. 150
170 m) then dividing by the depth of integration.

171 The net $bSiO_2$ production rate (ρ_N) was measured by the net change in biogenic silica
172 concentrations during incubations. During PB08, two 2.8 L polycarbonate bottles were filled
173 from each of the nine light depths sampled on rate casts and processed following the protocol
174 from Demarest et al. (2011). Briefly, one was assigned as the initial and immediately processed,
175 while the other was incubated for 24 hours and then processed. To account for $bSiO_2$ that
176 adsorbed to the bottle wall (Krause *et al.*, 2010b) each sample bottle was rinsed with three
177 aliquots of 0.2-μm-filtered seawater and the rinses passed through the same filter as the main
178 sample. Because of the low [$bSiO_2$] and the small net changes observed during PB08, the
179 protocol of Krause et al. (2010b) was used during PB09, where four replicates were run as initial
180 samples and another four incubated as final samples. The increased processing time limited
181 experiments to four depths (59, 31, 10, and 3.4% I_0). All samples were analyzed for both $bSiO_2$
182 and lithogenic silica, using NaOH – HF serial digestion described above, and corrected for bias
183 assuming that 10% of the lithogenic silica dissolves during the NaOH digestion (Ragueneau and
184 Treguer, 1994).

185 The export of $bSiO_2$ (ρ_E) at 150 m and 300 m was measured on PB08 using a free-drifting
186 Multitrap sediment trap array (e.g. Karl *et al.*, 1996). During the PB09 cruise the combined
187 factors of the passage of hurricane Felicia and occupying an active bloom area for <24 hours,
188 meant that sediment traps could not be deployed. On PB08, collector tubes fitted with entrance
189 baffles were filled with brine (50 g L^{-1} NaCl in 0.2 μm filtered surface seawater) and formalin
190 preservative was added to half the tubes. Three tubes of each type were deployed at 150 m and
191 300 m for approximately 5 days inside and outside of the bloom region. Samples were taken to
192 measure the amount of $bSiO_2$ which dissolved during deployment (~3% of particulate flux), as
193 described in Brzezinski et al. (2011), and used to correct the total measured $bSiO_2$ flux.
194 Dissolution was not measured in the preserved traps, but there was no significant difference

between the particulate flux in preserved and non-preserved traps deployed at the same depth and time (t-test, p values ranged 0.27 – 0.91 for pairwise comparisons).

3. Results

3.1. Hydrography and nutrients

The hydrography observed during each cruise is described briefly for context; however, a more thorough description can be found in Villareal et al. (2012). During PB08, MODIS imagery revealed a bloom feature developing to the northeast of Hawaii, near the subtropical front. CTD casts in the bloom region revealed significant small-scale salinity variations in vertical profiles (Fig. 2A, see also Villareal *et al.*, 2012) that are characteristic of the front (Shcherbina *et al.*, 2009, 2010). Isotherms in the upper 100 m showed little vertical variability at most stations on both transects, but some shoaling of the isothermal surfaces was observed in the lower-salinity stations presumably associated with the front (Fig. 2A). The mixed-layer depth in the bloom region averaged 21±7 m (SD).

Prior to PB09, MODIS satellite data revealed a bloom feature near 26°N and 145°W, which began developing in mid-June. By the time of our occupation, the satellite ocean color signal faded considerably and in situ measurements indicated that the bloom had collapsed. During a zonal transect across the former bloom region the water column had less temperature and salinity variability (Fig. 3A) than was observed during the PB08 transects, and the mixed layer was 40±13 m. A smaller and higher [Chl *a*] bloom was observed to develop closer to Hawaii, and reached the threshold bloom [Chl *a*] value by 7 August. Two rate stations (Sta. 22, 23) were occupied within this active bloom on 12 August, and satellite imagery showed it collapsed by 24 August. The physical conditions were similar to those observed in the collapsed-bloom region sampled during PB09, but the mixed layer depth was deeper, 48 – 50 m.

Consistent with gyre conditions, the concentrations of inorganic nutrients were very low at all stations. $[Si(OH)_4]$ in the surface waters was consistently one or two orders of magnitude higher than the high-sensitivity analysis concentrations for nitrate (<0.01 μM) and soluble reactive phosphate (<0.035 μM). On PB08, $[Si(OH)_4]$ was generally < 2 μM in the upper 50 m and the silicicline shoaled towards the north (Fig. 2C). At the single PB08 bloom station, the average mixed layer $[Si(OH)_4]$ showed a depletion to 1.22 μM and the vertical gradient in silicic acid from the base of the mixed layer to the 1% light depth was similar to that at the northern-

transect stations (Fig. 4A). Mixed-layer [$Si(OH)_4$] at non-bloom stations was 1.69±0.20 μM, implying a biological drawdown of ~0.5 μM [$Si(OH)_4$] in the bloom.

Dissolved silicate was consistently lower during the PB09 cruise (Fig. 3C). [$Si(OH)_4$] in the upper 50 m on the collapsed-bloom transect was <1.4 μM, and surface [$Si(OH)_4$] was <1 μM at some stations. In the active bloom, the average mixed-layer [$Si(OH)_4$] was 0.87 μM, ~0.3 μM less than that at non-bloom stations (Table 1). The vertical structure in [$Si(OH)_4$] below the mixed layer was similar at all stations during PB09 (bloom and non-bloom, Fig. 3C).

3.2. Particle concentrations and diatom abundance

Proxies for phytoplankton biomass showed expected low-levels outside of blooms and enhancement within blooms. We describe water-column [Chl *a*] (data not shown) for context and report integrated concentrations (Table 1), for a more thorough analysis of the [Chl *a*] dataset see Villareal et al. (2012). Total [Chl *a*] (i.e. >0.4 μm size fraction) was typically 0.15 – 0.25 μg L^{-1} in the deep chlorophyll maxima (~80 – 120 m) during both years. Higher values in the overlying waters were observed in PB08 (0.08 – 0.10 μg L^{-1}) vs. PB09 (<.08 μg L^{-1}). At the PB08 bloom station, the total [Chl *a*] showed relatively minor enhancement over concentrations at non-bloom stations. [Chl *a*] was >0.39 μg L^{-1} in the active PB09 bloom, with exceptionally high values of 0.54 and 1.03 μg L^{-1} observed between 45 and 55 m at stations 22 and 23, respectively. On average, the >10 μm fraction was ≤10% of the total [Chl *a*] in non-bloom stations during both years. However, this larger size fraction represented 30 – 40% of the total [Chl *a*] for PB08 bloom and 80 – 99% at station 23 in the active PB09 bloom.

Biogenic silica concentrations were consistent with previous studies in this region. [$bSiO_2$] at non-bloom stations during PB08 were 20 – 40 nmol Si L^{-1} in the upper 50 m (Fig. 2D). [$bSiO_2$] maxima, up to 100 nmol Si L^{-1}, were observed between 25 – 50 m at some stations on both transects. At the PB08 bloom station, the [$bSiO_2$] surpassed 200 nmol Si L^{-1} in the surface (Fig. 4B). [$bSiO_2$] along the PB09 transect of the faded bloom were between 10 and 20 nmol Si L^{-1} with little vertical structure in the euphotic zone (Fig. 3D). But in the active PB09 bloom, the [$bSiO_2$] was an order of magnitude higher than at non-bloom stations, with subsurface maximums of 153 and 240 nmol Si L^{-1} at stations 22 and 23, respectively (Fig. 4B).

Vertical integrals of biomass measurements reveal large differences between bloom and non-bloom stations during the PB cruises. During PB08 ∫Chl *a* within the >10 μm size fraction nearly

257 doubled at the single bloom station (2.5 mg m^{-2}), while ∫Chl *a* in the >0.4 μm size fraction at the
258 bloom station (18.3 mg m^{-2}) was similar to the non-bloom station average (18.8 mg m^{-2}, Table
259 1). During PB09, ∫Chl *a* in the >10 μm size fraction was 1.1 mg m^{-2} at the non-bloom stations
260 (includes profiles in the faded bloom) and significantly lower than the >0.4 μm size fraction
261 value (16.1 mg m^{-2}, Table 1). But within the active PB09 bloom, substantial increases were
262 observed in both size fractions; the >10 μm and >0.4 μm fractions averaged 18.3 mg m^{-2} and
263 53.5 mg m^{-2}, respectively (Table 1). Vertical integrals of [$bSiO_2$] showed relative changes
264 similar to those of >10 μm ∫Chl *a*, with significant differences between bloom and non-bloom
265 stations. During PB08, the non-bloom ∫$bSiO_2$ averaged 40% of the bloom station value (13.3
266 mmol Si m^{-2}, Table 1). Similarly, the non-bloom ∫$bSiO_2$ in PB09 was only 26% of the ∫$bSiO_2$ at
267 the two active bloom stations during PB09 (7.7 mmol Si m^{-2}, Table 1).
268 Diatom abundance and species dominance differed between cruises. During PB08,
269 *Hemiaulus hauckii* was the numerically dominant diatom at all stations (Table 1). The vertical
270 structure in diatom abundance (Fig. 2B, 3B, 4F) was similar to that for [$bSiO_2$] (Figs. 2D, 3D,
271 4B) and >10 μm [Chl *a*] (Fig. 4C). Surface maximums of ~250 cells L^{-1} were observed during
272 the PB08 transects, with abundances <50 cells L^{-1} persisting deeper than 50 m (Fig. 2B). Diatom
273 abundance increased to >10,000 cells L^{-1} in the surface at the bloom station, with >100 cells L^{-1}
274 at depths shallower than 60 m (Fig. 4F). The integrated diatom abundance within the mixed-
275 layer varied by an order of magnitude between non-bloom (5.9 $x10^6$ cells m^{-2}) and bloom
276 stations (8.2 $x10^7$ cells m^{-2}, Table 1). *M. woodiana* dominated abundance at 11 of the 14 stations
277 where abundance data was obtained during PB09, with *H. hauckii* and *Chaetoceros* spp. being
278 most abundant diatoms at the other stations (Table 1). Non-bloom station cell abundance was
279 very low, e.g. <50 cells L^{-1}, with little vertical structure (Fig. 3B). Within the active bloom, *M.*
280 *woodiana* accounted for 98% of total diatom abundance, despite maximum numerical
281 abundances for all diatom genera being observed in this bloom (Table 1). Maximum diatom cell
282 abundances in the station-22 mixed layer were 38,000 cells L^{-1}, and maximum mixed-layer
283 abundances were higher at station 23 (159,000 cells L^{-1}, Fig. 4F). The mixed-layer integrated
284 diatom abundance at non-bloom stations during PB09 (1.1 $x10^6$ cells m^{-2}) was three orders of
285 magnitude lower than at the active bloom stations (1.4 $x10^9$ cells m^{-2}; Table 1).
286
287 *3.3. Biogenic silica production and export rates*

Gross biogenic silica production rates (ρ_P) varied by an order of magnitude between bloom and non-bloom stations. Surface ρ_P ranged between 2 – 5 nmol Si L^{-1} d^{-1} at non-bloom stations during PB08 (Fig. 2E) and increased to >20 nmol Si L^{-1} d^{-1} at the bloom station (Fig. 4D). Vertical trends in ρ_P below 50 m were similar in and out of the bloom area, with rates declining from <1 nmol Si L^{-1} d^{-1} at 50 m to analytically zero at 175 m, indicating that the full vertical extent of ρ_P in the water column was sampled (Fig. 2E). At PB09 non-bloom stations, only two samples (out of 59) had rates >2 nmol Si L^{-1} d^{-1}. Rates in the upper 50 m were generally 1.2 – 1.8 nmol Si L^{-1} d^{-1} and below 50 m, deep ρ_P declined to rates similar to rates observed in PB08 (Fig. 3E). Within the active PB09 bloom, ρ_P values were >15 nmol Si L^{-1} d^{-1} throughout the upper 50 m, with a subsurface maximum of 54 nmol Si L^{-1} d^{-1} (Fig. 4D). Deeper than 60 m, ρ_P at the active bloom stations were nearly identical to those rates measured at non-bloom stations. Vertical integrals of ρ_P ($\int\rho_P$) demonstrate the strong disparity between bloom and non-bloom rates. Non-bloom station average $\int\rho_P$ during PB08 was 32% of the bloom-station rate (0.65 mmol Si m^{-2} d^{-1}, Table 1). A larger disparity was observed in PB09, as the non-bloom average $\int\rho_P$ was only 9% of the active bloom rate (1.33 mmol Si m^{-2} d^{-1}).

As with ρ_P, [$bSiO_2$], and diatom abundance, specific uptake rate V_b was generally highest in the upper water column and declined to analytical zero values at the 0.1%I_0 isolume (Fig. 2F, 3F, 4E). During PB08, V_b in the upper 15 m were ~0.05 – 0.08 d^{-1} at non-bloom stations (Fig. 2F), but at the bloom station V_b in the upper 15 m was ~0.11 d^{-1} (Fig. 4E), implying doubling times of ~6 and ~10 days inside and outside bloom, respectively. Vertically-weighted average V_b within the upper 150 m showed no difference between the non-bloom (0.05 d^{-1}) and bloom (0.04 d^{-1}) rates (Table 1), indicating an average doubling time for $bSiO_2$ in the upper 150 m of approximately two weeks during the PB08 cruise. V_b on the faded-bloom transect during PB09 was >0.05 d^{-1} in the upper 50 m at two stations and values ≥0.05 d^{-1} throughout the upper 150 m at the easternmost station (Fig. 3F). At the active-bloom stations during PB09, V_b averaged ~0.35 d^{-1} in the upper 10 m with a maximum of 0.75 d^{-1} at the base of the mixed layer (~50 m, Fig. 4E); the latter infers a doubling time of <1 day. For PB09, the vertically-averaged V_b within the active bloom (0.17 d^{-1}) was nearly three-fold higher than for non-bloom stations (0.06 d^{-1}), implying doubling times of 4 and 11 days for bloom and non-bloom stations, respectively.

The net production of biogenic silica (ρ_N) is defined as the difference between ρ_P and gross silica dissolution, and thereby represents an upper limit for $bSiO_2$ export. Because ρ_N was not sampled at every rate station during PB08, we do not have a measurement at the single bloom station. When integrated within the mixed layer, $\int\rho_N$ was positive at three stations (Fig. 5). Integration to deeper depths (e.g. 3.4%I_0 and 0.1%I_0) caused $\int\rho_N$ to become negative, indicating that within the euphotic zone the dissolution of $bSiO_2$ exceeded its rate of production. During PB09, replication allowed for constraints on the variability in the estimates of $\int\rho_N$ (Fig. 5B). Nearly all stations showed positive $\int\rho_N$ over the mixed layer and often between the surface and the 3.4%I_0 isolume (Fig. 5), but only in the active bloom (stations 22, 23, Fig. 5) was $\int\rho_N$ statistically different from zero (i.e. production of $bSiO_2$ exceeded its loss from dissolution) for the mixed layer and to the 3.4%I_0 isolume integrals. Considering the variability among replicated samples during PB09, $\int\rho_N$ measured during PB08 were unlikely to be statistically different from zero. These results suggest that the outside of bloom stations, silica production and dissolution were approximately in balance leading to no or very little net silica production (i.e. $\int\rho_N \approx 0$) within the mixed layer.

Due to inclement weather, no sediment trap deployments were made during PB09; however, we can make comparisons between bloom and non-bloom regions for $bSiO_2$ flux (ρ_E) during PB08. Samples with and without formalin showed no statistically significant difference in the measured ρ_E (t-test, p values ranged 0.27 – 0.91), and we report the pooled mean ±SD from both trap types. ρ_E at 150 m within the bloom area was higher than that observed outside the bloom (0.27 ±0.05 mmol Si m^{-2} d^{-1} vs. 0.17 ±0.03 mmol Si m^{-2} d^{-1}). Unexpectedly, ρ_E at 300 m in the bloom area was 0.36 ±0.03 mmol Si m^{-2} d^{-1}, ~33% higher than ρ_E at 150 m in the bloom, and was four-fold higher than 300-m ρ_E outside the bloom (0.09 ±0.01 mmol Si m^{-2} d^{-1}).

4. Discussion

4.1. Siliceous biomass and silica production during summer in the NPSG

The blooms sampled during the PB cruises are similar to summer-period stocks and rates observed previously in this region. On zonal transects along ~25°N and 31°N in NPSG during summer, Brzezinski et al. (1998) observed a $\int bSiO_2$ range of 2 – 18 mmol Si m^{-2} (Fig. 6A), but

by our diatom-bloom criteria only one bloom station was sampled during their cruises. Between 1997 and 2009, summer blooms occurred most years at station ALOHA, elevating $\int bSiO_2$ by ~50% above the non-summer average (2.5 mmol Si m^{-2}; Brzezinski *et al.*, 2011). The PB08 bloom-station $\int bSiO_2$ (Table 1) was similar to the highest values observed in all 12 years of $bSiO_2$ data at station ALOHA, but about 33% lower than the highest integrals reported by Brzezinski et al. (1998) (Fig. 6A). Similarly, the $\int bSiO_2$ at the PB09 active bloom stations (Table 1) was comparable to the highest values observed in the ALOHA record (Fig. 6A). Non-bloom station $\int bSiO_2$ during the PB cruises (Table 1) was also similar to values during previous studies in this region (Fig. 6A). Combining our data with the previous data at station ALOHA and from transects by Brzezinski et al. (1998) shows that the magnitude of $\int bSiO_2$ during the summer season does not appear to increase from the gyre interior (near ALOHA) to the northeastern boundary (near the subtropical front).

Reports of biogenic silica production rates in the NPSG are limited. Brzezinski et al. (1998) reported $\int \rho_P$ between 0.5 and 2.9 mmol Si m^{-2} d^{-1} (average 1.2 mmol Si m^{-2} d^{-1}) during their summer cruises in the mid-1990s (Fig. 6B). This range and mean were significantly higher than that observed recently at station ALOHA, where non-summer $\int \rho_P$ ranged between 0.1 – 0.2 mmol Si m^{-2} d^{-1} and summer values averaged 0.4 mmol Si m^{-2} d^{-1} (Fig. 6B; Brzezinski *et al.*, 2011). $\int \rho_P$ at the three PB bloom stations was higher than at ALOHA during the summer (Brzezinski *et al.*, 2011) and they were similar to the mean rate reported for all stations by Brzezinski et al. (1998) (Fig. 6B). One other report of biogenic silica production rates in this region was for *Rhizosolenia* mats during the summer months (Shipe *et al.*, 1999). Shipe et al. (1999) estimated that *Rhizosolenia* mat production was up to ~0.3 mmol Si m^{-2} d^{-1} in the upper 150 m. This rate surpasses nearly all non-bloom stations during the PB cruises (Table 1) and reinforces Shipe et al.'s (1999) conclusions that *Rhizosolenia* mats are an important overlooked source of silica production in this region.

4.2. Comparison to other open-ocean diatom blooms

Even under bloom conditions, the diatom biomass in the NSPG is lower than coastal zones (Brzezinski *et al.*, 1997; 2003; Shipe and Brzezinski, 2001) or the Southern Ocean/Antarctica (Nelson *et al.*, 1991) and this results in significantly lower rates of $bSiO_2$ production (Table 2). Consequently, NSPG gross rates are low and similar in magnitude to other subtropical gyres.

However, the elevated rates observed in the PB blooms are comparable to those observed in subtropical-gyre mesoscale features, where intensified vertical nutrient supply enhances phytoplankton rate processes (e.g. McGillicuddy *et al.* 1998). NPSG blooms are distinct for being spatially larger (Table 2) and for occurring without significant enhancement of macronutrients by obvious mesoscale processes. In the Sargasso Sea, Krause et al. (2010b) observed greatly enhanced [$bSiO_2$], $\int\rho_P$ and $\int\rho_N$ in a mode-water eddy (MWE), the same eddy type harboring the enhanced diatom community described by McGillicuddy et al. (2007). While $\int bSiO_2$ was higher in the MWE than at all PB stations, $\int\rho_P$ was similar and the total amount of $bSiO_2$ produced in this MWE may have been similar to that observed in the PB09 bloom (Table 2). But $\int\rho_N$ was nearly 3-fold higher in the PB09 bloom compared to the MWE. Eddies have also been observed to have enhanced diatom biomass relative to normal (e.g. non-bloom) conditions in the NPSG (Benitez-Nelson *et al.*, 2007; Fong *et al.*, 2008), but direct comparison with the PB blooms is problematic since no measurements of [$bSiO_2$] and silica production were made during these studies. However, Benitez-Nelson et al. (2007) did report a 150-m ρ_E of 0.43 mmol Si m^{-2} d^{-1} in an NPSG cyclonic eddy (i.e. "Cyclone Opal"), this value is only 20% higher than the 300-m ρ_E measured in PB08 bloom region (Fig. 6C).

Compared to other diatom blooms examined to date, the PB09 bloom appeared to have lower proportional losses of biogenic silica due to silica dissolution. The ratio of net $bSiO_2$ accumulation relative to the gross rate ($\int\rho_N \div \int\rho_P$) is equivalent to the statistic 1 – D:P, a diagnostic of fraction of "new" silica production (Brzezinski *et al.*, 2003) (D:P is the ratio of gross silica dissolution to gross silica production). In the PB09, the 1 – D:P in the active bloom was 0.77, this is higher than other blooms in subtropical gyres (e.g. 0.66; Krause *et al.*, 2010b) and is similar to bloom values observed in high-diatom biomass systems including the Gulf Stream Warm Core Rings, Antarctic Polar Front, and the Amazon River Plume (*see* fig. 4 in Brzezinski *et al.* 2003). Thus, in the active PB09 bloom, the much lower proportional loss of $bSiO_2$ due to dissolution allows for a higher fraction of ρ_P to result in $\int bSiO_2$ accumulation and potentially export.

4.3. Bloom drivers

The summer blooms in the NPSG have been shown to be quantitatively significant in terms of their effect on the annual export of particulate organic matter to the ocean interior (Scharek *et*

409 *al.*, 1999b; Dore *et al.*, 2008; Karl *et al.*, 2012); however, a consensus view as to what is driving
410 blooms during this period has yet to be realized. A companion study suggested that Si was not
411 limiting to diatom growth during these blooms (Krause et al. 2012); therefore, input of Si can be
412 eliminated as a potential bloom driver. The increase in available N by enhanced nitrogen
413 fixation has been suggested to be a mechanism which facilitates blooms in the NPSG (e.g.
414 Wilson, 2003; Dore *et al.*, 2008); such that blooms of diazotrophs or DDAs would be regulated
415 more by nutrients such as phosphorus and iron (e.g. Calil *et al.*, 2011). This did not seem to be
416 the case during PB08. A study of phosphorus cycling by Duhamel et al., (2010) found little
417 evidence of P limitation during PB08 leading to the suggestion that the autotrophs present were
418 mainly limited by N, thus giving direct advantage to organisms capable of N_2 fixation. This is
419 consistent with the finding that *H. hauckii*, a DDA, dominated the PB08 diatom silica biomass
420 and silica production rates (Krause *et al.*, 2012). However, N_2 fixation rates measured on the
421 cruise were quite low. Watkins-Brandt et al. (2011) report the highest N_2 fixation rates on this
422 cruise to be ~2 nmol N L^{-1} d^{-1}, with most values being ≤1 nmol N L^{-1} d^{-1}. Considering an average
423 diatom Si:N of 1:1 (Brzezinski, 1985) and the maximizing assumption that all measured N_2
424 fixation was solely by DDAs, then the measured N_2 fixation rates by Watkins-Brandt et al.
425 (2011) could potentially support most silica production at non-bloom stations, but <10% of silica
426 production rates measured at the PB08 bloom station.
427 The dominant diatom in the active bloom on PB09, *M. woodiana*, is not a DDA and thus
428 does not benefit directly from N_2 fixation. *M. woodiana* has been observed on multiple
429 occasions to be a numerically dominant diatom in NPSG blooms (see table 1 in Dore *et al.* 2008)
430 despite its small size, it also has been observed to be high abundance in local sediment traps
431 (Scharek *et al.*, 1999a; b), possibly because of its ability to form large aggregates (Villareal *et*
432 *al.*, 2012). Both *M. woodiana* and DDAs are part of the same near-surface flora (Venrick, 1988),
433 suggesting that *M. woodiana* benefits from an indirect linkage with coexisting DDAs where food
434 web processes, or direct N excretion, transfer N from DDAs to non-nitrogen fixers, but the role
435 of such processes in bloom initiation and/or development remains unclear (Villareal *et al.*, 2012).
436 Other mechanisms that may drive blooms are physical, including mesoscale features
437 (Church *et al.*, 2009) and fronts (Calil and Richards, 2010). In a synthesis of four blooms
438 sampled in the northeastern sector of the NPSG (including the two blooms reported here),
439 Wilson et al. (in review) suggest that bloom development requires a subsurface stratification

minimum intersecting the nutricline and that this is close to the base of the mixed layer. However, this assumes that biological productivity in blooms is driven by N_2 fixation (i.e. solitary/colonial diazotrophs or DDA) making biological production limited by P availability. Wilson (2011) recently presented a hypothesis to explain blooms occurring to the northeast of Hawaii near the subtropical front where internal waves, generated at the Hawaiian islands, propagate to the northeast and break near a "critical latitude" (e.g. 30° N), thereby enhancing vertical mixing across the nutricline. The PB08 bloom was located very near the "critical latitude."

4.4. Bloom dynamics

Multiple lines of evidence suggest the PB08 bloom region was sampled while in a declining state. The MODIS satellite data showed that surface [Chl *a*] had started declining in this feature prior to our sampling. The bloom had [Chl *a*] above the 0.12 μg L^{-1} threshold through at least 8 July 2008, although due to cloud coverage much of the feature was obscured from MODIS during its decline. The bloom station was sampled on 9 July; thus, most of our stations were sampled after the bloom was below the ocean-color bloom threshold. Evidence of bloom decline was also apparent by a lack of significant differences in V_b between the PB08 bloom and those at some non-bloom stations (Fig. 2, 3, Table 1), indicating low diatom activity in the declining bloom. Lastly, there was a lack of vertical attenuation of ρ_E in the bloom. The export at 300 m was 33% higher than that at 150 m, whereas outside the bloom the $bSiO_2$ flux at 300 m was half of the flux at 150 m. Given the temporal lag for particles exported at 150 m to reach 300 m, the increase in flux with depth suggests that a large pulse of silica export occurred prior to our occupation.

In contrast to the PB08 bloom, nearly every measurement taken supports that the active PB09 bloom was sampled in a state of rapid autotrophic-biomass accumulation. The MODIS data indicates that stations 22 and 23 were sampled at the peak biomass achieved by this bloom (Villareal *et al.*, 2012). The ρ_P and V_b observed in this bloom were the highest of all stations during both PB cruises and were comparable to the highest rates observed at station ALOHA during two years of study (2008 – 2009; Brzezinski *et al.*, 2011). The high specific production rates imply doubling-time estimates within the PB09 active bloom to be <1 – 2 days in the upper 55 m, relative to the 10 – 14 day doubling times elsewhere. This evidence suggests a highly

dynamic diatom community, despite the predominant condition of very low [NO_3], [SRP] (i.e. no different than non-bloom stations), which was still in a state of positive net $bSiO_2$ production during our sampling, notwithstanding the even lower [$Si(OH)_4$] than non-bloom station (presumably from biological drawdown).

A distinction among the three bloom stations sampled on the PB cruises is the shift in numerical dominance by different diatom genera among blooms and their implied contribution to silicon dynamics. Recently, we used a biovolume scaling approach (sensu Conley *et al.*, 1989) to determine the Si quota of the dominant diatoms in the PB blooms to estimate which diatom species likely dominated ρ_P and the community V_b (Krause *et al.*, 2012). We observed that *H. hauckii* and *M. woodiana* dominated the PB08 and active PB09 blooms, respectively, and they likely dominated ρ_P due to the combined effects of each group having the highest contribution to [$bSiO_2$] and highest net growth rates, compared to the other diatoms present. Thus, in these blooms it appears that numerical dominance by a particular diatom group also resulted in those groups having the most significant role in local silicon biogeochemistry. Such a condition is not always true among diatom assemblages, as a recent analysis in the eastern equatorial Pacific suggested that up to 40% of the $\int\rho_P$ in the euphotic zone was done by diatoms representing <10% of the total abundance (Krause *et al.*, 2010a).

The export of biogenic silica in the PB08 bloom was significant in the context of the regional dataset. Biogenic silica flux at 150 m has been regularly sampled by the HOT program since 1997 (Brzezinski *et al.*, 2011) where ρ_E is ~0.07 mmol Si m^{-2} d^{-1} and ~0.13 mmol Si m^{-2} d^{-1} during non-summer and summer months, respectively (Fig. 6C). During the PB08 cruise, ρ_E within and outside of the bloom region were both enhanced, relative to average rates observed at station ALOHA (Fig. 6C). The 300-m ρ_E of 0.36 mmol Si m^{-2} d^{-1} within the PB08 bloom area is higher than all but two of the 87 cruise values reported for 150 m ρ_E at ALOHA since 2001 (Brzezinski *et al.*, 2011) and was 85% of the 150-m ρ_E observed at in a regional cyclonic eddy ("Cyclone Opal") which harbored significantly enhanced diatom biomass (Benitez-Nelson *et al.*, 2007). Under steady-state conditions, the $\int\rho_N$ measurement sets an upper limit for export. At most stations, positive $\int\rho_N$ was observed in the mixed layer, with increasingly negative values for deeper integral depths (Fig. 5). Such biomass accumulation, and export potential, in the mixed layer, suggests that diatoms in the NPSG may operate in reverse of the classical two-layer model

(Dugdale, 1967; Eppley *et al.*, 1973), where export originates in the deeper layer from phytoplankton having adequate nutrients but are limited by light.

During the PB cruises we can adequately resolve differences in net production between the bloom and non-bloom stations but the method has high uncertainty due to natural variability in $bSiO_2$ replicates. At station ALOHA, an average of 54% of total integrated silica production is available for export (i.e. net production) (Brzezinski *et al.*, 2011); however, the absolute export rates were low (see previous paragraph). With the high uncertainty in the $\int\rho_N$ measurement, such a small positive signal in $\int\rho_N$ (inferred by the station ALOHA dataset) at non-bloom stations cannot be resolved. Only in the active PB09 bloom was $\int\rho_N$ positive and statistically different from zero, suggesting that during this bloom there was an increased decoupling between production and dissolution of silica, relative to that observed under non-bloom conditions, this decoupling lead to higher net accumulation of biomass and high export potential. The observation that *M. woodiana* formed visible aggregates in this bloom (Villareal *et al.*, 2012) provides a mechanism to enhance the settling rate of these diatoms, relative to the rate for single cells, thereby enabling *M. woodiana* to be important in export (*M. woodiana* and *H. hauckii* numerically dominate diatom flux at ALOHA during summer; Scharek *et al.*, 1999b). The PB09-bloom $\int\rho_N$ implies a maximum potential for export of 1.1 mmol Si m^{-2} d^{-1}, which ~40% higher than the highest ρ_E observed in this region (Fig. 6C), and consistent with diatom export during summer blooms being important to regional carbon export (Karl *et al.*, 2012).

4.5. The potential summer bloom effect on the annual Si budget in the NPSG

During 2008 and 2009 at station ALOHA, blooms accounted for 29% of annual $\int\rho_P$ (Brzezinski *et al.*, 2011). This percentage is based on average daily rates of 0.4 mmol Si m^{-2} d^{-1} during two summer-period blooms. Incorporating the $\int\rho_P$ from the active PB09 bloom (~ same latitude as ALOHA; Fig. 1) into the Brzezinski et al. (2011) average, increases the bloom-average $\int\rho_P$ from 0.4 mmol Si m^{-2} d^{-1} to 0.63 mmol Si m^{-2} d^{-1} or by nearly 50%. Based on the limited number of diatom blooms sampled at or near station ALOHA, the contribution of blooms to annual silica production rates calculated by Brzezinski et al. (2011) may be conservative.

Calculating the contribution of blooms to annual budgets requires their total silica production, frequency, and areal extent. Bloom frequency and areal extent are best obtained from satellite ocean color recognizing the limitations of linking DDA-diatom blooms to ocean

color (Villareal *et al.*, 2011; 2012). The PB08 bloom had remotely-observed [Chl *a*] of >0.12 μg L^{-1} over an average area of 100,000 km^2. The active PB09 bloom had significantly higher silica production but covered only 30,000 km^2. Both blooms persisted ~16 days but during this time period cloud cover sometimes obscured the bloom, introducing a likely error of at least a few days. Using the $\int\rho_P$ for the bloom stations (e.g. PB09 average 1.33 mmol Si m^{-2} d^{-1}), we estimate that the PB08 and PB09 blooms produced 1.04 and 0.64 Gmoles of $bSiO_2$, respectively (Table 2). For comparison, non-bloom rates expressed over this same area and duration would yield 0.21 and 0.12 Gmoles of $bSiO_2$ for PB08 and PB09, respectively. Due to their tremendous areal extent, these blooms also are significant when considering blooms in other high diatom biomass regions (e.g. Monterey Bay, Santa Barbara Channel; Table 2). And, while the PB09 bloom was much more biologically active by all our proxies, the larger size of the PB08 bloom more than offset the difference in production rates and suggests even diffuse blooms significantly affect regional Si budgets. A caveat to these estimations is that the blooms were clearly sampled in different stages of their development; therefore, the amount of biogenic silica produced in the PB08 bloom is likely underestimated, especially given the higher reported $\int\rho_P$ by Brzezinski et al. (1998) in this sector of the NPSG during summer (Fig. 6B).

Wilson et al. (2008) demonstrated that blooms in the northeastern quadrant of the NPSG, near the subtropical front, are significantly larger in area (up to five-fold) and have longer duration than blooms near station ALOHA (i.e. gyre-interior). MODIS [Chl *a*] data between June and October of 2008 and 2009 show strong differences in the extent of blooms in each year of our field study (Fig. 7). A caveat to our analysis is the large amount of cloud cover obscured the study region; therefore, the days a particular location was above our threshold [Chl *a*] (color scale, Fig. 7A, B) are conservative for all areas. By averaging the $\int\rho_P$ from all three bloom stations during the PB cruises (0.99 mmol Si m^{-2} d^{-1}), and assuming a 10-day duration (minimum estimate based on MODIS data, Fig. 7A, B) we can extrapolate for the $bSiO_2$ produced during the 2008 and 2009 bloom seasons in three latitudinal bands (Fig. 7C, Table 2). In both years, the majority of silica production occurred between 30 – 35°N (Table 2). Overall, in 2008 and 2009 the northern latitude blooms (e.g. 30 – 35 °N) produced 3x and 25x more $bSiO_2$ than blooms in the gyre interior (e.g. 20 – 25 °N), as a function of the larger bloom area during both years. Given the differences in the size and duration between blooms in the northeastern portion of the gyre and those in the interior near station ALOHA (e.g. Fig. 7), the gyre-interior blooms would

have to sustain $\int \rho_P$ nearly an order of magnitude faster than rates in the north to produce more $bSiO_2$ than the northeastern-gyre blooms (Table 2). Considering that the PB08 bloom rate, even under declining conditions, was 49% of the rate observed in the active PB09 bloom, this seems unlikely. While the contribution of diatoms to silica and organic matter production and export is well documented at station ALOHA in the gyre interior (Scharek *et al.*, 1999a; b; Brzezinski *et al.*, 2011; Karl *et al.*, 2012) this analysis suggests that the role of diatom blooms to these processes is even greater in the northeastern reaches of the gyre near the subtropical front.

The temporal resolution of studies reporting Si biogeochemical data in the NSPG outside of station ALOHA is very poor, and not conducive for constructing an annual budget. The northeastern region of the NPSG near the subtropical front zone may operate differently in regards to annual rates of silica production and export than in the gyre interior near station ALOHA as a consequence of spatially-larger and longer-persisting blooms (Wilson *et al.*, 2008). Here we demonstrate that there is significant spatial variation in siliceous biomass and production rates in the NSPG during the summer, which may be of biogeochemical importance for a regional Si budget and especially to annual rates diatom silica and carbon export. The northeastern region of the NPSG near the subtropical front, where the most expansive blooms occur, is not amenable to monthly sampling as is done at station ALOHA. However, future studies in this and other sectors of the NPSG, could examine processes such export by using passive (e.g. sediment traps) methods or autonomous vehicles (e.g. glider with fluorometer and/or transmissometer) which sample with higher temporal resolution.

Acknowledgements

We thank J. Jones, E. Allman, C. Beucher, C. Brown, D. Foley, V. Franck, J. Goodman, A. Pyle, K. Rogers, K. Swanson, and S. Vega for logistical and technical assistance, M. Church and S. Duhamel for data access, the Captain, resident technicians and crew of the R/V *Kilo Moana* for assistance at sea. This work was funded by National Science Foundation Ocean Sciences grants OCE-0648130 awarded to MAB, and OCE-0726726 and OCE-0094591 awarded to TAV.

591

592 **References**

593

594 Arrigo, K.R., van Dijken, G.L., 2004. Annual changes in sea-ice, chlorophyll a, and primary
595 production in the Ross Sea, Antarctica. Deep-Sea Research II 51, 117-138.
596 Benitez-Nelson, C.R., Bidigare, R.R., Dickey, T.D., Landry, M.R., Leonard, C.L., Brown, S.L.,
597 Nencioli, F., Rii, Y.M., Maiti, K., Becker, J.W., Bibby, T.S., Black, W., Cai, W.J., Carlson,
598 C.A., Chen, F.Z., Kuwahara, V.S., Mahaffey, C., McAndrew, P.M., Quay, P.D., Rappe,
599 M.S., Selph, K.E., Simmons, M.P., Yang, E.J., 2007. Mesoscale eddies drive increased silica
600 export in the subtropical Pacific Ocean. Science 316 (5827), 1017-1021.
601 doi:10.1126/science.1136221
602 Brzezinski, M.A., 1985. The Si:C:N ratio of marine diatoms: Interspecific variability and the
603 effect of some environmental variables. Journal of Phycology 21 (3), 347-357.
604 Brzezinski, M.A., Jones, J.L., Bidle, K.D., Azam, F., 2003. The balance between silica
605 production and silica dissolution in the sea: Insights from Monterey Bay, California, applied
606 to the global data set. Limnology and Oceanography 48 (5), 1846-1854.
607 Brzezinski, M.A., Krause, J.W., Church, M.J., Karl, D.M., Li, B., Jones, J.L., Updyke, B., 2011.
608 The annual silica cycle of the North Pacific subtropical gyre. Deep-Sea Research I 58 (10),
609 988-1001. doi:10.1016/j.dsr.2011.08.001
610 Brzezinski, M.A., Nelson, D.M., 1995. The annual silica cycle in the Sargasso Sea near
611 Bermuda. Deep-Sea Research I 42 (7), 1215-1237.
612 Brzezinski, M.A., Phillips, D.R., 1997. Evaluation of Si-32 as a tracer for measuring silica
613 production rates in marine waters. Limnology and Oceanography 42 (5), 856-865.
614 Brzezinski, M.A., Phillips, D.R., Chavez, F.P., Friederich, G.E., Dugdale, R.C., 1997. Silica
615 production in the Monterey, California, Upwelling System. Limnology and Oceanography
616 42 (8), 1694-1705.
617 Brzezinski, M.A., Villareal, T.A., Lipschultz, F., 1998. Silica production and the contribution of
618 diatoms to new and primary production in the central North Pacific. Marine Ecology-
619 Progress Series 167, 89-104.

620 Calil, P.H.R., Doney, S.C., Yumimoto, K., Eguchi, K., Takemura, T., 2011. Episodic upwelling
621 and dust deposition as bloom triggers in low-nutrient, low-chlorophyll regions. Journal of
622 Geophysical Research-Oceans 116 (C06030). doi:10.1029/2010jc006704
623 Calil, P.H.R., Richards, K.J., 2010. Transient upwelling hot spots in the oligotrophic North
624 Pacific. Journal of Geophysical Research-Oceans 115. doi:10.1029/2009jc005360
625 Church, M.J., Mahaffey, C., Letelier, R.M., Lukas, R., Zehr, J.P., Karl, D.M., 2009. Physical
626 forcing of nitrogen fixation and diazotroph community structure in the North Pacific
627 subtropical gyre. Global Biogeochemical Cycles 23. doi:10.1029/2008gb003418
628 Conley, D.J., Kilham, S.S., Theriot, E., 1989. Differences in silica content between marine and
629 fresh-water diatoms. Limnology and Oceanography 34 (1), 205-213.
630 Demarest, M.S., Brzezinski, M.A., Nelson, D.M., Krause, J.W., Jones, J.L., Beucher, C.P., 2011.
631 Net biogenic silica production and nitrate regeneration determine the strength of the silica
632 pump in the Eastern Equatorial Pacific. Deep-Sea Research II 58 (3-4), 462-476.
633 doi:10.1016/j.dsr2.2010.08.007
634 Dore, J.E., Letelier, R.M., Church, M.J., Lukas, R., Karl, D.M., 2008. Summer phytoplankton
635 blooms in the oligotrophic North Pacific Subtropical Gyre: Historical perspective and recent
636 observations. Progress in Oceanography 76 (1), 2-38. doi:10.1016/j.pocean.2007.10.002
637 Dugdale, R.C., 1967. Nutrient limitation in the sea: dynamics, identification, and significance.
638 Limnology and Oceanography 12 (4), 685-695.
639 Duhamel, S., Bjorkman, K.M., Wambeke, F.V., Moutin, T., Karl, D.M., 2011. Characterization
640 of alkaline phosphatase activity in the North and South Pacific Subtropical Gyres:
641 Implications for phosphorus cycling. Limnology and Oceanography 56 (4), 1244-1254.
642 doi:10.4319/lo.2011.56.4.1244
643 Duhamel, S., Dyhrman, S.T., Karl, D.M., 2010. Alkaline phosphatase activity and regulation in
644 the North Pacific Subtropical Gyre. Limnology and Oceanography 55 (3), 1414-1425.
645 doi:10.4319/lo.2010.55.3.1414
646 Eppley, R.W., Renger, E.H., Venrick, E.L., Mullin, M.M., 1973. A study of plankton dynamics
647 and nutrient cycling in the central gyre of the North Pacific ocean. Limnology and
648 Oceanography 18 (4), 534-551.

649 Fong, A.A., Karl, D.M., Lukas, R., Letelier, R.M., Zehr, J.P., Church, M.J., 2008. Nitrogen
650 fixation in an anticyclonic eddy in the oligotrophic North Pacific Ocean. Isme Journal 2 (6),
651 663-676. doi:10.1038/ismej.2008.22
652 Karl, D.M., Christian, J.R., Dore, J.E., Hebel, D.V., Letelier, R.M., Tupas, L.M., Winn, C.D.,
653 1996. Seasonal and interannual variability in primary production and particle flux at Station
654 ALOHA. Deep-Sea Research II 43 (2-3), 539-568.
655 Karl, D.M., Church, M.J., Dore, J.E., Letelier, R.M., Mahaffey, C., 2012. Predictable and
656 efficient carbon sequestration in the North Pacific Ocean supported by symbiotic nitrogen
657 fixation. PNAS 109 (6), 1842-1849. doi:10.1073/pnas.1120312109
658 Krause, J.W., Brzezinski, M.A., Jones, J.L., 2011. Application of low level beta counting of 32Si
659 for the measurement of silica production rates in aquatic environments. Marine Chemistry
660 127, 40-47. doi:10.1016/j.marchem.2011.07.001
661 Krause, J.W., Brzezinski, M.A., Landry, M.R., Baines, S.B., Nelson, D.M., Selph, K.E., Taylor,
662 A.G., Twining, B.S., 2010a. The effects of biogenic silica detritus, zooplankton grazing, and
663 diatom size structure on silicon cycling in the euphotic zone of the eastern equatorial Pacific.
664 Limnology and Oceanography 55 (6), 2608-2622. doi:10.4319/lo2010.55.6.2608
665 Krause, J.W., Brzezinski, M.A., Villareal, T.A., Wilson, C., 2012. Increased kinetic efficiency
666 for silicic acid uptake as a driver of summer diatom blooms in the North Pacific Subtropical
667 Gyre. Limnology and Oceanography 57 (4).
668 Krause, J.W., Nelson, D.M., Lomas, M.W., 2009. Biogeochemical responses to late-winter
669 storms in the Sargasso Sea, II: Increased rates of biogenic silica production and export. Deep-
670 Sea Research I 56 (6), 861-874. doi:10.1016/j.dsr.2009.01.002
671 Krause, J.W., Nelson, D.M., Lomas, M.W., 2010b. Production, dissolution, accumulation and
672 potential export of biogenic silica in a Sargasso Sea mode-water eddy. Limnology and
673 Oceanography 55 (2), 569-579.
674 McGillicuddy, D.J., Anderson, L.A., Bates, N.R., Bibby, T., Buesseler, K.O., Carlson, C.A.,
675 Davis, C.S., Ewart, C., Falkowski, P.G., Goldthwait, S.A., Hansell, D.A., Jenkins, W.J.,
676 Johnson, R., Kosnyrev, V.K., Ledwell, J.R., Li, Q.P., Siegel, D.A., Steinberg, D.K., 2007.
677 Eddy/Wind Interactions Stimulate Extraordinary Mid-Ocean Plankton Blooms. Science 316
678 (5827), 1021-1026.

679 McGillicuddy, D.J., Robinson, A.R., Siegel, D.A., Jannasch, H.W., Johnson, R., Dickeys, T.,
680 McNeil, J., Michaels, A.F., Knap, A.H., 1998. Influence of mesoscale eddies on new
681 production in the Sargasso Sea. Nature 394 (6690), 263-266.
682 Nelson, D.M., Ahern, J.A., Herlihy, L.J., 1991. Cycling of biogenic silica within the upper water
683 column of the Ross Sea. Marine Chemistry 35, 461-476.
684 Ragueneau, O., Treguer, P., 1994. Determination of biogenic silica in coastal waters -
685 applicability and limits of the alkaline digestion method. Marine Chemistry 45 (1-2), 43-51.
686 doi:10.1016/0304-4203(94)90090-6
687 Scharek, R., Latasa, M., Karl, D.M., Bidigare, R.R., 1999a. Temporal variations in diatom
688 abundance and downward vertical flux in the oligotrophic North Pacific gyre. Deep-Sea
689 Research I 46 (6), 1051-1075.
690 Scharek, R., Tupas, L.M., Karl, D.M., 1999b. Diatom fluxes to the deep sea in the oligotrophic
691 North Pacific gyre at Station ALOHA. Marine Ecology Progress Series 182, 55-67.
692 Shcherbina, A.Y., Gregg, M.C., Alford, M.H., Harcourt, R.R., 2009. Characterizing
693 Thermohaline Intrusions in the North Pacific Subtropical Frontal Zone. Journal of Physical
694 Oceanography 39 (11), 2735-2756. doi:10.1175/2009jpo4190.1
695 Shcherbina, A.Y., Gregg, M.C., Alford, M.H., Harcourt, R.R., 2010. Three-Dimensional
696 Structure and Temporal Evolution of Submesoscale Thermohaline Intrusions in the North
697 Pacific Subtropical Frontal Zone. Journal of Physical Oceanography 40 (8), 1669-1689.
698 doi:10.1175/2010jpo4373.1
699 Shipe, R.F., Brzezinski, M.A., 2001. A time series study of silica production and flux in an
700 eastern boundary region: Santa Barbara Basin, California. Global Biogeochemical Cycles 15
701 (2), 517-531.
702 Shipe, R.F., Brzezinski, M.A., Pilskaln, C., Villareal, T.A., 1999. Rhizosolenia mats: An
703 overlooked source of silica production in the open sea. Limnology and Oceanography 44 (5),
704 1282-1292.
705 Sverdrup, H.U., 1953. On Conditions for the Vernal Blooming of Phytoplankton. ICES Journal
706 of Marine Science 18 (3), 287-295.
707 Venrick, E.L., 1988. The vertical distributions of chlorophyll and phytoplankton species in the
708 North Pacific central environment. Journal of Plankton Research 55, 987-998.

709 Venrick, E.L., 1997. Comparison of the phytoplankton species composition and structure in the
710 Climax area (1973-1985) with that of station ALOHA (1994). Limnology and Oceanography
711 42 (7), 1643-1648.
712 Villareal, T.A., Adornato, L., Wilson, C., Schoenbaechler, C.A., 2011. Summer blooms of
713 diatom-diazotroph assemblages and surface chlorophyll in the North Pacific gyre: A
714 disconnect. Journal of Geophysical Research-Oceans 116 (C03001), 15.
715 doi:10.1029/2010jc006268
716 Villareal, T.A., Brown, C.G., Brzezinski, M.A., Krause, J.W., Wilson, C., 2012. Summer Diatom
717 Blooms in the North Pacific Subtropical Gyre: 2008–2009. PLoS One 7 (4), e33109.
718 doi:10.1371/journal.pone.0033109
719 Watkins-Brandt, K.S., Letelier, R.M., Spitz, Y.H., Church, M.J., Boettjer, D., White, A.E., 2011.
720 Addition of inorganic or organic phosphorus enhances nitrogen and carbon fixation in the
721 oligotrophic North Pacific. Marine Ecology Progress Series 432, 17-29.
722 doi:10.3354/meps09147
723 Welschmeyer, N.A., 1994. Fluorometric analysis of chlorophyll a in the presence of chlorophyll
724 b and pheopigments. Limnology and Oceanography 39 (8), 1985-1992.
725 Wilson, C., 2003. Late Summer chlorophyll blooms in the oligotrophic North Pacific Subtropical
726 Gyre. Geophysical Research Letters 30 (18). doi:10.1029/2003gl017770
727 Wilson, C., 2011. Chlorophyll anomalies along the critical latitude at 30 degrees N in the NE
728 Pacific. Geophysical Research Letters 38. doi:10.1029/2011gl048210
729 Wilson, C., Villareal, T.A., Brzezinski, M.A., Krause, J.W., Shcherbina, A.Y., in review.
730 Chlorophyll bloom development and the Subtropical Front in the North Pacific.
731 Wilson, C., Villareal, T.A., Maximenko, N., Bograd, S.J., Montoya, J.P., Schoenbaechler, C.A.,
732 2008. Biological and physical forcings of late summer chlorophyll blooms at 30 degrees N in
733 the oligotrophic Pacific. Journal of Marine Systems 69 (3-4), 164-176.
734 doi:10.1016/j.jmarsys.2005.09.018

735 Figure Captions:

736

737 Fig. 1: Station locations during the PB08 and PB09 cruises, station ALOHA (HOT program) is
738 shown for reference. Symbols are distinguished by year (PB08, circles; PB09, squares) and
739 bloom stations (filled symbols). Outlined regions are the maximum areal extent of the MODIS-
740 defined bloom regions (>0.12 μg L^{-1} [Chl *a*]). Transect direction is denoted by arrows.

741

742 Fig. 2: Section plots showing hydrography, nutrients and biological properties with depth during
743 the PB08 transects near the subtropical front. A) Salinity and temperature (contours), B) diatom
744 abundance, C) dissolved silicate concentration, D) biogenic silica concentration [$bSiO_2$], E)
745 biogenic silica production, ρ_P and F) specific biogenic silica production, V_b. The bloom station
746 data is not shown as it was situated slightly west of transect 1 (see Fig. 1).

747

748 Fig. 3: Section plots showing hydrography, nutrients and biological properties with depth during
749 the PB09 transect. Panels and scales are as in Figure 2. Bloom stations were located far west of
750 this transect and are not shown (see Fig. 4).

751

752 Fig. 4: Vertical profiles of nutrients and biological properties at the PB bloom stations. Each
753 bloom station is distinguished by symbol type: PB08 (black), PB09 St. 22 (gray crossed), PB09
754 St. 23 (gray). For comparison, non-bloom (N.B.) station data were binned by depth, averaged,
755 and plotted (depth is the midpoint of the bin) for PB08 (black line) and PB09 (gray line).

756

757 Fig. 5: The net production of $bSiO_2$ ($\int\rho_N$) during A) PB08 and B) PB09. Bars represent vertical
758 integrals based either in the mixed layer or to a specific light depth. *Indicates bloom station
759 during PB09, the PB08 bloom station was not sampled. Error bars are propagated from the
760 measured variance in the replicates, and summed with depth.

761

762

763 Fig. 6: Comparison of A) $\int bSiO_2$, B) $\int \rho_P$, and C) 150-m $bSiO_2$ export in the NPSG. The square
764 symbols and error bars are the average and standard deviation, respectively, filled symbols
765 represent data range. Data are arranged by non-summer (September through May) and summer
766 (bloom season, June through August) months. Data is from Brzezinski et al. (2011) (station
767 ALOHA), Brzezinski et al. (1998) (transects north of ALOHA during August 1995, July 1996),
768 and this study; "nd" indicates no data. The PB08 bloom export value at 300 m is averaged with
769 the flux values at 150 m from in and out of the bloom area (total of three data points).

770

771 Fig. 7: Comparison of 2008 and 2009 bloom seasons in the NPSG using the MODIS dataset. A,
772 B) days where daily [Chl *a*] was >0.12 μg L^{-1} for 2008 (A) and 2009 (B) between June and
773 October. C) The area (km^2) where [Chl *a*] was >0.12 μg L^{-1}; values were binned by latitude and
774 represent the same time period and data from A, B. The longitude considered was between 180–
775 130° W, except for the 30 – 35° N bin where the only data between 180–135°W was used (to
776 avoid the California Current boundary). Note: because these use daily MODIS values, the
777 duration of each bloom is potentially underestimated due to cloud cover (i.e. days with no
778 recorded value), this is the case for the PB09 bloom feature which was only successfully viewed
779 during five different days, albeit over a 16-day span.

780

781 Highlights:
782 • Bloom biogenic silica stocks and production were enhanced by an order of magnitude
783 • Bloom biogenic silica export at 300 m was among the highest values in the region
784 • 77% of gross silica production in one bloom accumulated as biomass (54% is normal)
785 • Northeastern blooms potentially produced 3–25x more silica than gyre-interior blooms
786

Table 1

Table 1: Mixed layer depth (MLD), dissolved silicate, biological and particulate data for the PB cruises. All integrations are to 150 m (common depth for all stations and generally shallower than the 0.1% light depth) except for the total diatoms (MLD integration). V_b is average in the upper 150 m (see Methods). Note: integration depths for diatoms, Chl *a* and $bSiO_2$ differ from those presented in Villareal et al. (2012), as their study focused on surface flora (i.e. 0 – 60 m).

Cruise	Station	Lat. (°N)	Long. (°W)	MLD (m)	MLD Ave. $[Si(OH)_4]$ (µM)	MLD ∫Diatoms (10^6 m^{-2})	Dominant Diatom (%)	∫$bSiO_2$ (mmol m^{-2})	∫Chl *a*, >0.4µm (mg m^{-2})	∫Chl *a*, >10µm (mg m^{-2})	$\int\rho_P$ (mmol Si m^{-2} d^{-1})	Ave. V_b (d^{-1})
PB08	1	30.00	150.00	23.3	1.90	6.27	*Hemiaulus* (69)	2.34	17.1	1.21	0.19	0.08
PB08	2	30.00	146.50	35.0	1.60	10.6	*Hemiaulus* (64)	3.06	14.4	1.10	0.19	0.05
PB08	3	32.35	140.86	11.5	1.67	4.90	*Hemiaulus* (89)	7.18	17.9	1.35	0.25	0.03
PB08	4	32.06	140.67	22.0	1.63	—	—	9.16	20.1	1.71	—	—
PB08	5	31.77	140.47	11.8	1.93	8.32	*Hemiaulus* (46)	6.16	17.7	1.26	0.18	0.03
PB08	6	31.48	140.28	15.0	1.95	—	—	3.80	21.4	1.61	—	—
PB08	*7	31.77	140.71	11.3	1.22	82.9	*Hemiaulus* (97)	12.83	18.3	2.50	0.65	0.04
PB08	8	31.67	140.92	13.0	1.39	—	—	6.85	21.7	2.01	—	—
PB08	9	31.19	140.08	27.3	1.55	8.29	*Hemiaulus* (90)	6.27	17.1	1.36	0.22	0.04
PB08	10	30.90	139.89	25.0	1.62	—	—	5.33	19.0	1.33	—	—
PB08	12	30.61	139.70	24.5	1.53	3.46	*Hemiaulus* (83)	5.48	17.3	1.35	0.10	0.02
PB08	13	30.32	139.51	14.0	1.66	—	—	5.23	19.1	1.44	—	—
PB08	14	28.75	141.25	21.3	1.50	2.26	*Hemiaulus* (89)	5.11	15.8	1.81	0.25	0.06
PB08	15	31.52	140.58	24.7	1.68	—	—	6.74	18.4	1.54	0.30	0.04
PB08	16	32.00	139.00	24.0	2.06	1.06	*Hemiaulus* (81)	3.67	19.2	1.75	0.20	0.06
PB08	17	31.67	139.33	22.0	2.10	0.25	*Hemiaulus* (99)	2.79	20.8	1.63	—	—
PB08	18	31.33	139.67	26.0	1.68	10.6	*Hemiaulus* (98)	3.69	19.9	1.63	—	—
PB08	19	31.00	140.01	21.0	1.49	12.5	*Hemiaulus* (97)	5.08	20.1	1.69	—	—
PB08	20	30.67	140.34	12.0	1.58	4.06	*Hemiaulus* (99)	2.66	19.4	1.52	—	—
PB08	21	30.33	140.67	22.0	1.60	3.93	*Hemiaulus* (~100)	~	20.2	1.59	—	—
PB09	1	20.50	153.69	34.5	1.19	3.79	*Mastogloia* (73)	2.12	21.0	1.88	0.15	0.07
PB09	2	25.20	147.00	28.0	1.04	1.01	*Mastogloia* (36)	1.80	16.5	1.37	—	—
PB09	†3	26.10	144.70	43.0	0.99	0.99	*Mastogloia* (67)	2.11	17.7	1.09	0.10	0.05
PB09	†4	26.10	144.35	37.0	1.02	0.49	*Mastogloia* (64)	1.91	18.8	1.71	—	—
PB09	†7	26.10	144.00	49.0	0.86	0.25	*Mastogloia* (49)	2.03	4.68	0.31	0.10	0.05
PB09	†8	26.10	143.65	42.0	1.03	0.69	*Hemiaulus* (34)	1.57	16.0	0.95	—	—
PB09	†11	26.10	143.30	43.5	1.32	0.56	*Mastogloia* (74)	1.77	16.4	0.93	0.12	0.07
PB09	†12	26.10	142.95	8.0	1.34	0.20	*Mastogloia* (~100)	1.80	15.3	0.80	—	—
PB09	13	25.48	143.00	36.8	1.02	1.27	*Hemiaulus* (55)	1.99	14.7	0.93	0.13	0.06
PB09	†15	26.10	142.60	40.0	1.37	—	—	2.04	15.0	0.76	—	—

PB09	†16	26.10	142.25	58.0	1.02	—	—	2.24	17.1	1.20	—	—
PB09	†17	26.10	141.90	34.5	1.28	2.46	*Mastogloia* (56)	2.34	20.9	1.39	—	—
PB09	†18	26.10	141.55	48.0	1.26	0.89	*Mastogloia* (86)	2.05	15.2	0.94	—	—
PB09	20	27.50	142.00	37.0	1.30	—	—	2.54	15.7	1.00	—	—
PB09	21	23.50	140.00	58.6	1.30	6.96	*Chaetoceros* (74)	1.69	17.6	1.18	0.10	0.06
PB09	*, ‡22	25.10	154.70	47.7	0.91	509	*Mastogloia* (98)	6.13	63.3	18.05	0.91	0.16
PB09	*, ‡23	25.18	154.60	52.7	0.82	2410	*Mastogloia* (99)	9.19	43.7	18.53	1.74	0.17

* Bloom stations (i.e. fulfilled data-based criteria)

† Faded bloom stations (PB09; 26°N, 145°W)

‡Integration depth ($0.1\%I_0$) was only 131 and 134 m for stations 22 and 23, respectively.

Table 2: Estimates for the amount of $bSiO_2$ produced by the individual blooms sampled in 2008 and 2009 (active bloom), and for the $bSiO_2$ produced during the bloom season (June-October) in three latitude bins, assuming a duration of 10 days (see Fig. 7). For comparison, we have included $bSiO_2$ produced in other regions using published bloom rates and also assuming a 10-day duration.

Bloom or Region	$\int\rho_P$ (mmol Si m^{-2} d^{-1})	Duration (days)	†Bloom Area (km^2)	$bSiO_2$ Produced (Gmoles)	Reference
PB08 bloom	0.65	16	100,000	1.04	This study
PB09 bloom	1.33	16	30,000	0.64	
NPSG 2008 bloom season					
20-25°N	0.99	10	234,798	2.32	This study
25-30°N	0.99	10	114,425	1.13	
30-35°N	0.99	10	758,114	7.51	
NPSG 2009 bloom season					
20-25°N	0.99	10	15,052	0.15	This study
25-30°N	0.99	10	57,156	0.57	
30-35°N	0.99	10	386,566	3.83	
Sargasso Sea: mode-water eddy	0.98	10	24,200	0.24	Krause *et al.*, 2010b
Monterey Bay	60	10	1,200	0.72	Brzezinski *et al.*, 1997, 2003
Santa Barbara Channel	40	10	4,200	1.68	Shipe and Brzezinski, 2001
Ross Sea polynya	34	10	‡160,000	54.4	Nelson *et al.*, 1991

†Bloom rate is assumed over the ***entire*** regional area

‡Average open water area (October - May) over nine years (Arrigo and van Dijken, 2004)

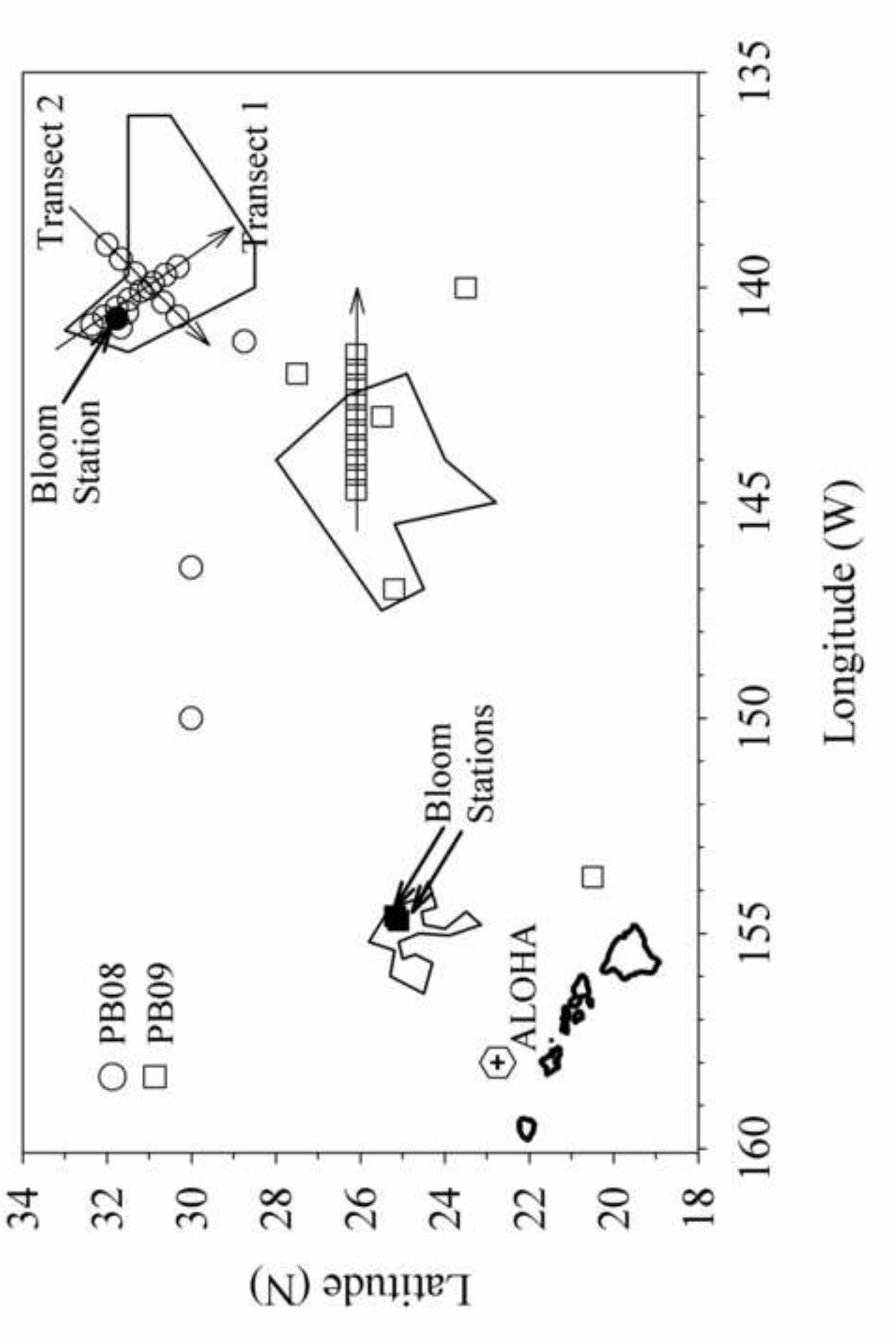

Figure 1

Figure 2

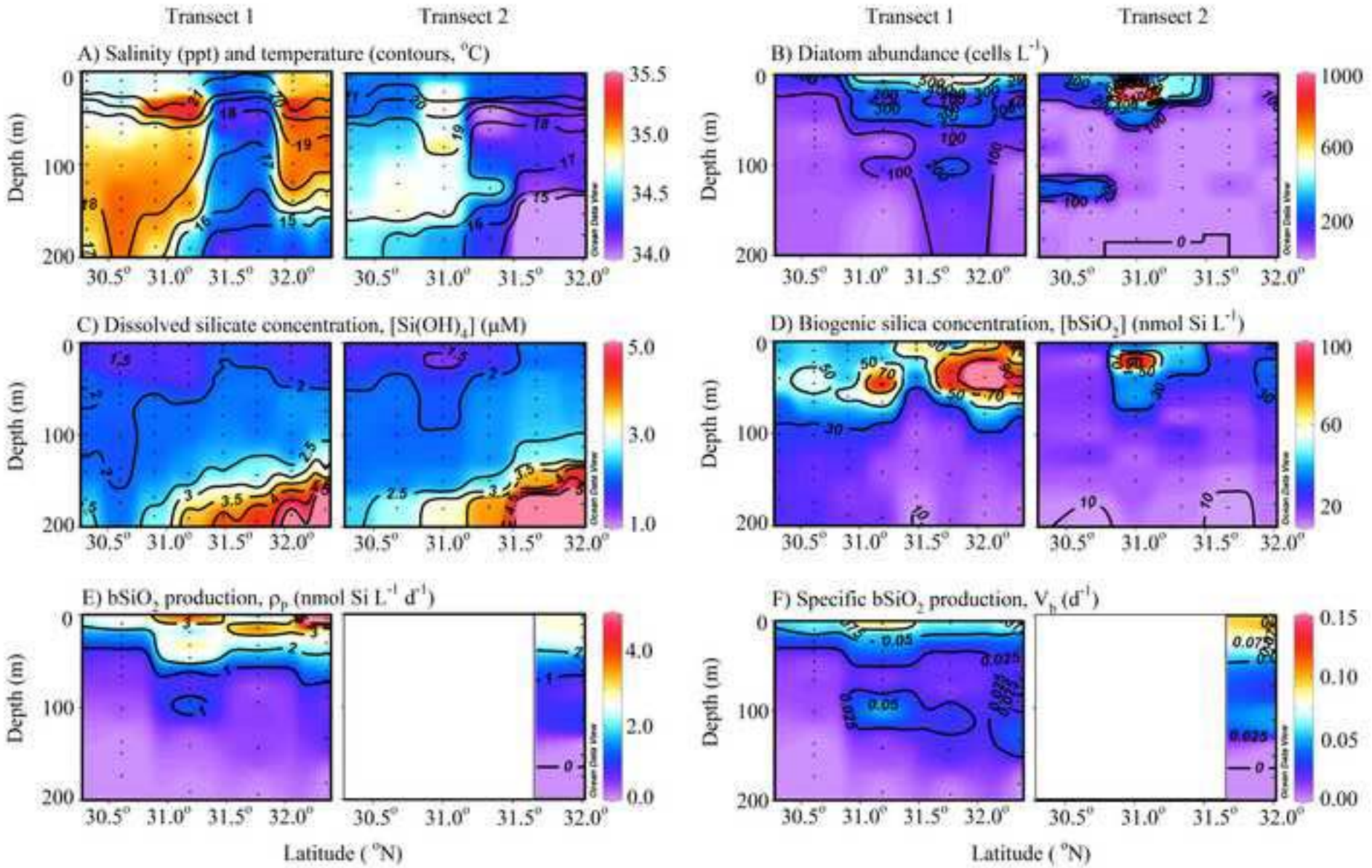

Figure 3

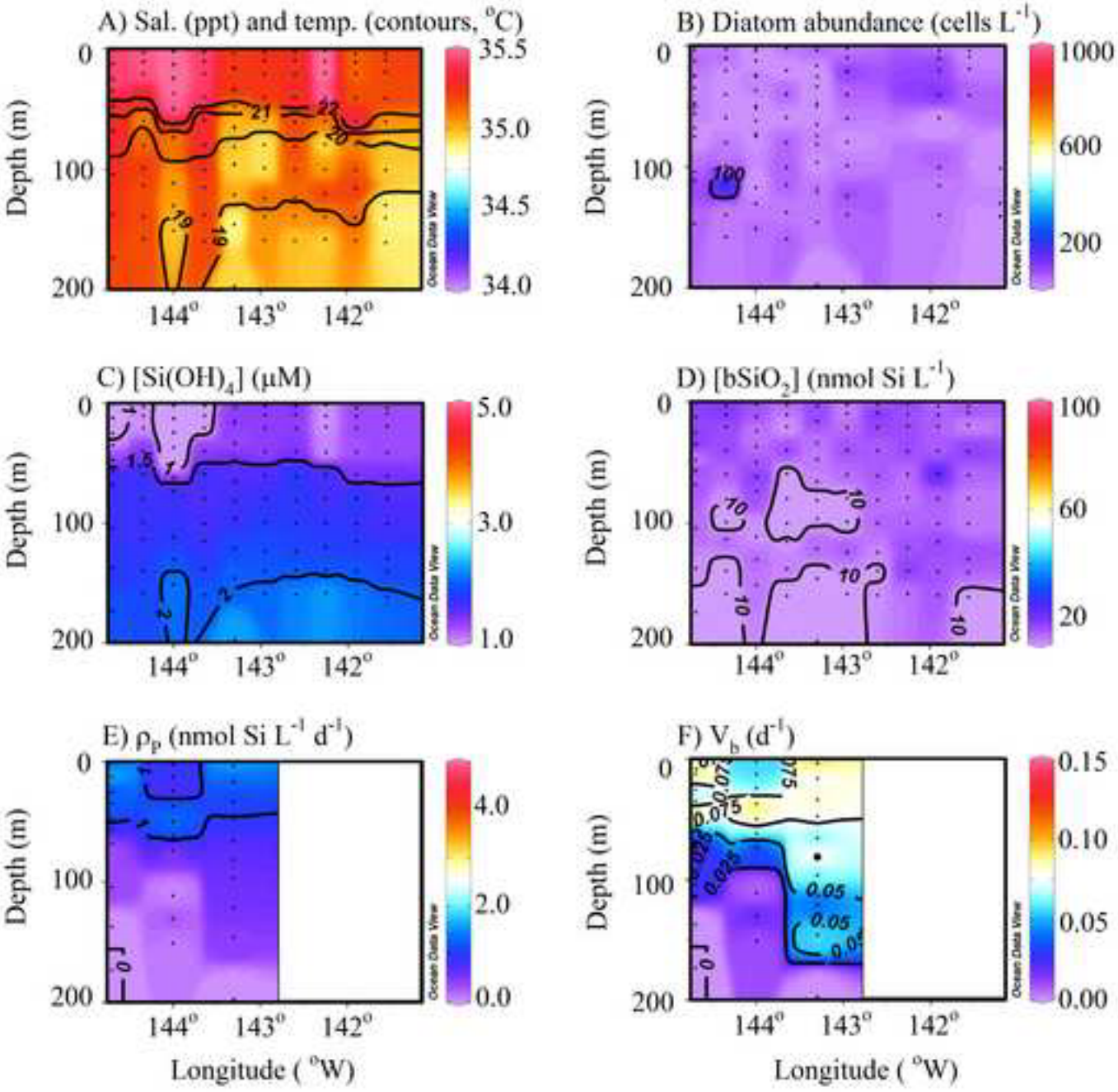

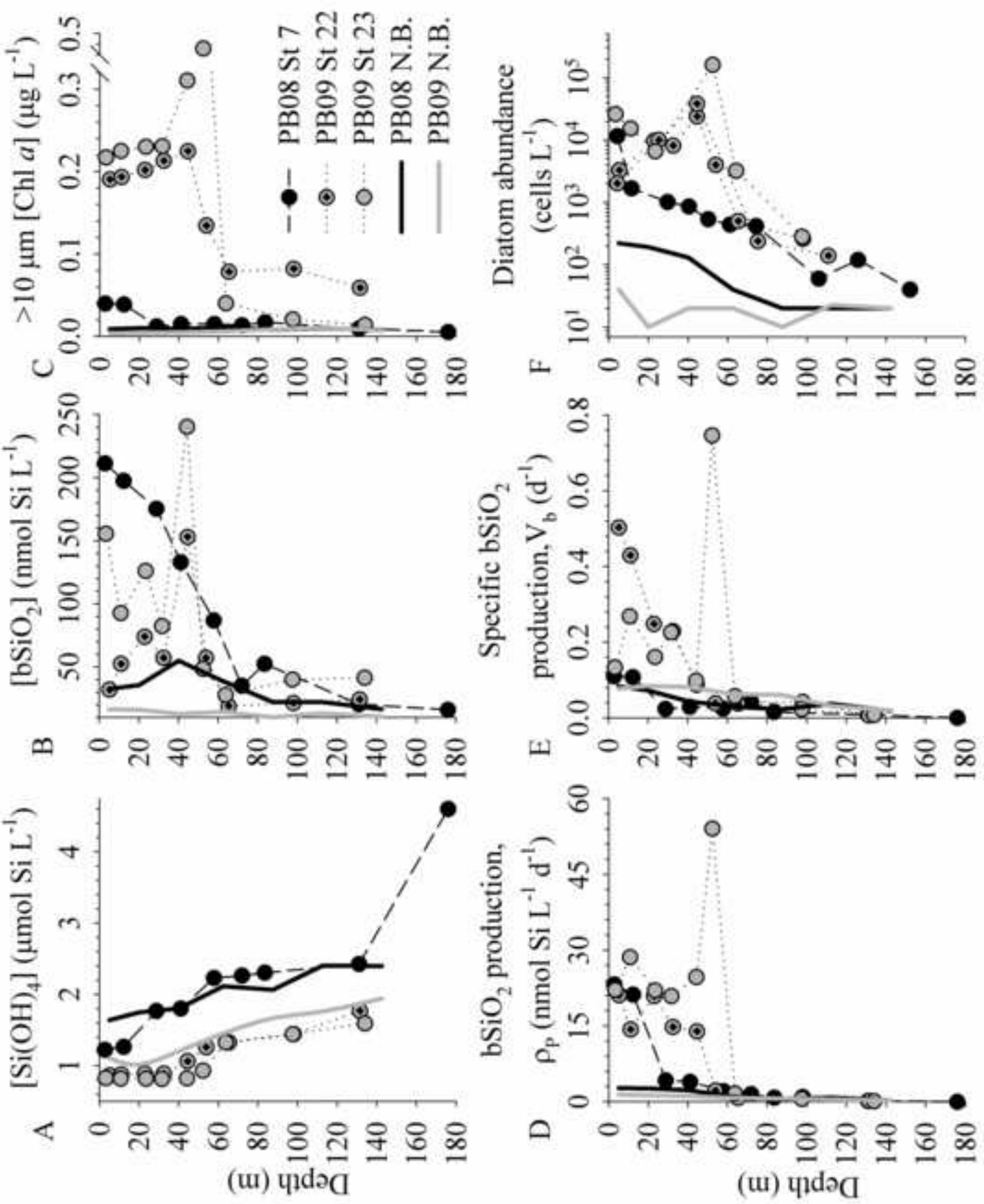
A
[Si(OH)4] (µmol Si L-1)
B
[bSiO2] (nmol Si L-1)
C
>10 µm [Chl a] (µg L-1)
PB08 St 7
PB09 St 22
PB09 St 23
PB08 N.B.
PB09 N.B.
D
bSiO2 production, ρP (nmol Si L-1 d-1)
E
Specific bSiO2 production, Vb (d-1)
F
Diatom abundance (cells L-1)
Depth (m)

Figure 4

Figure 5

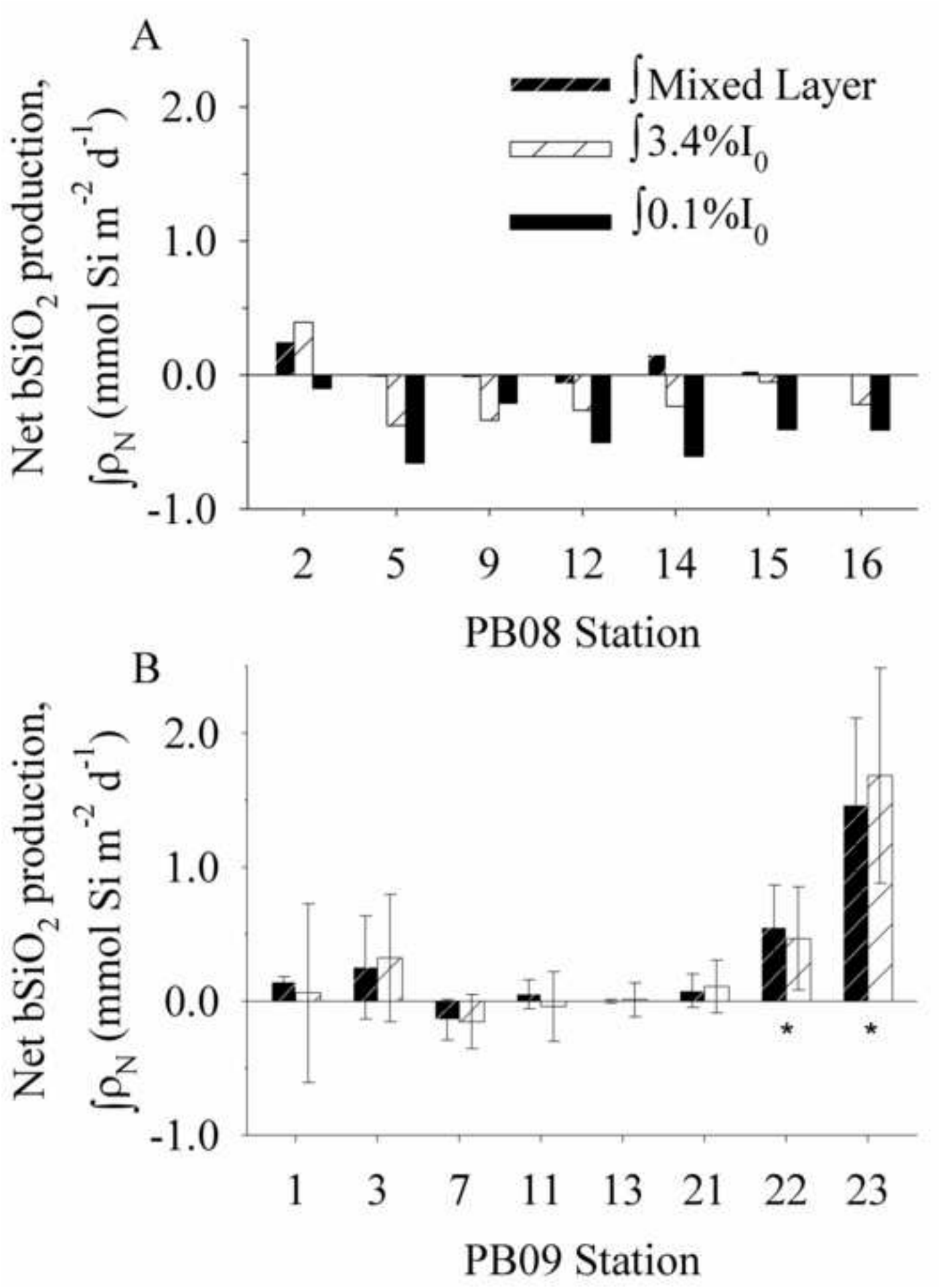

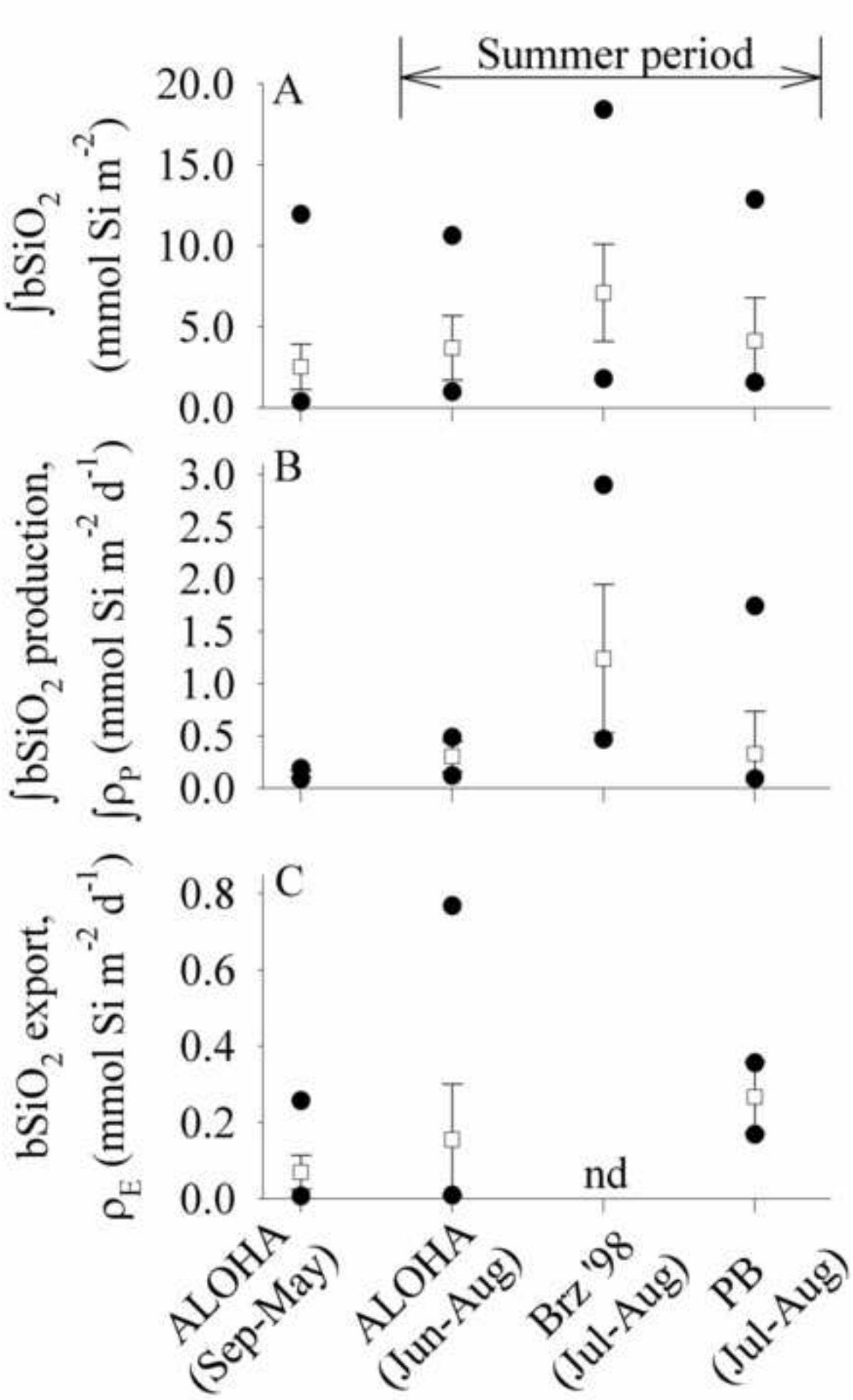

Figure 7